Photonic crystal gas sensors

Torsten M. Geppert, Stefan L. Schweizer, J. Schilling, Cecile Jamois, A. V. Rhein, et al.

Torsten M. Geppert, Stefan L. Schweizer, J. Schilling, Cecile Jamois, A. V. Rhein, D. Pergande, Regine Glatthaar, P. Hahn, A. Feisst, Armin Lambrecht, Ralf B. Wehrspohn, "Photonic crystal gas sensors," Proc. SPIE 5511, Tuning the Optical Response of Photonic Bandgap Structures, (14 October 2004); doi: 10.1117/12.561724

SPIE.

Event: Optical Science and Technology, the SPIE 49th Annual Meeting, 2004, Denver, Colorado, United States

Photonic crystal gas sensors

T.M. Geppert[a,b], S.L. Schweizer[b], J. Schilling[c], C. Jamois[a], A.v. Rhein[b], D. Pergande[b], R. Glatthaar[d], P. Hahn[d], A. Feisst[d], A. Lambrecht[d] and R.B. Wehrspohn[b]

[a] Max Planck Institute of Microstructure Physics, Weinberg 2, 06120 Halle (Saale), Germany;
[b] University Paderborn, Dept. Physics, Warburger Str. 100, 33098 Paderborn, Germany;
[c] Dept. of Electrical Engineering, California Institute of Technology, MC 136-93 Pasadena, CA 91125-9300, USA;
[d] Fraunhofer Institute for Physical Measurement Techniques, Heidenhofstr. 8, 79110 Freiburg, Germany

ABSTRACT

The bandstructure of photonic crystals offers intriguing possibilities for the manipulation of electromagnetic waves. During the last years, research has mainly focussed on the application of these photonic crystal properties in the telecom area. We suggest utilization of photonic crystals for sensor applications such as qualitative and quantitative gas and liquid analysis. Taking advantage of the low group velocity and certain mode distributions for some $\vec{k}$-points in the bandstructure of a photonic crystal should enable the realization of very compact sensor devices. We show different device configurations of a photonic crystal based on macroporous silicon that fulfill the demands to serve as a compact gas sensor.

Keywords: Photonic Crystals, sensor application, low group velocity, macroporous silicon

1. INTRODUCTION

1.1. Photonic Crystals

Photonic Crystals (PhCs) are the optical analog to electronic semiconductors, i.e., PhCs are *semiconductors* for photons. The concept of PhCs was introduced independently in 1987 by Sajeev John[1] and Eli Yablonovitch.[2]
In electronic semiconductors like Si or GaAs the bandstructure for the electrons arises from the periodic arrangement of the atoms that make up the crystal lattice. Electron waves travelling through the electronic semiconductor are scattered at the periodic electrostatic potentials of the atoms and their interference leads to the replacement of the free electron dispersion relation $E^{\text{free}}_{\text{electron}}(\vec{k}) = (\hbar^2\vec{k}^2)/(2m)$ by the electronic bandstructure.
In PhCs the photonic bandstructure (PhBS) results from scattering and interference of electromagnetic (em) waves at periodic arrangements of materials with different refractive indices $n = \sqrt{\epsilon}$, where ϵ is the materials dielectric constant. The PhBS replaces the dispersion relation of photons $\omega = (c/n)|\vec{k}|$ in a homogenous dielectric medium with refractive index n and frequency ω along the direction $\vec{k}$, where c is the speed of light in vacuum. The PhBS depends on several parameters.
One important parameter is the geometry of the lattice of the PhC. Fig.1 shows three out of many possible arrangements of a material with dielectric constant ϵ_2, e.g., air pores, in a host material with dielectric constant ϵ_1, such as, e.g., Si. Assuming that the diameter of the air pores in Fig.1 does not change along the z-axis, such a structure is called a two-dimensional (2D) PhC. If the pore diameter is varied along the z-axis in such a way, that there is in addition to the periodicity in the x-y-plane also a periodicity l_z along the z-direction, such a structure would be called a 3-dimensional (3D) PhC.
Another important parameter that influences the PhBS is the so-called dielectric contrast $\Delta\epsilon = \epsilon_1 - \epsilon_2$ which is significant in the case of the air/Si material system where one has $\Delta\epsilon_{\text{air,Si}} = \epsilon_{\text{Si}} - \epsilon_{\text{air}} = 11.6 - 1 = 10.6$. As a rule of thumb the photonic bandstructure shifts to higher frequencies and the photonic bandgap (PhBG) increases when the dielectric contrast is increased.

E-mail: tgeppert@mpi-halle.mpg.de, telephone: +49 (0)345 5582-901

Tuning the Optical Response of Photonic Bandgap Structures, edited by Philippe M. Fauchet, Paul V. Braun, Proceedings of SPIE Vol. 5511 (SPIE, Bellingham, WA, 2004) · 0277-786X/04/$15 · doi: 10.1117/12.561724

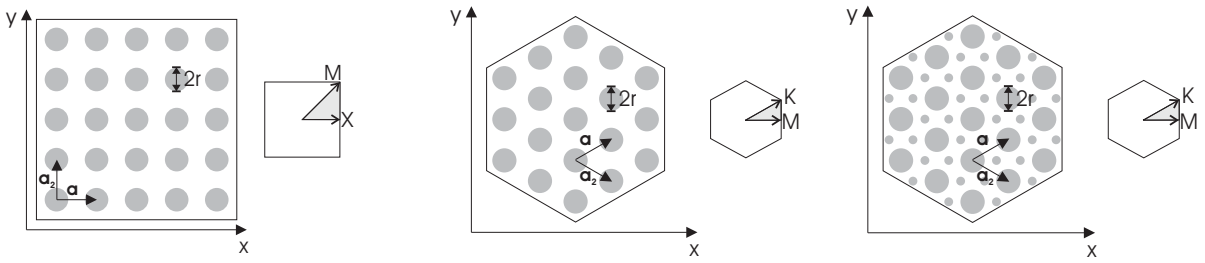

Figure 1. Arrangement of a material of dielectric constant ϵ_2 within a material of dielectric constant ϵ_1. This could be experimentally realized as, e.g., air pores along the z-direction in bulk Si. **(a)** Square lattice, **(b)** hexagonal lattice and **(c)** two-base hexagonal lattice. $\overrightarrow{a_1}$ and $\overrightarrow{a_2}$ represent basis vectors of the underlying PhC lattice. The righthand insets depict the corresponding Brillouin zones with points of high symmetry. The shaded region represents the irreducible Brillouin zone.

The PhBS depends furthermore on the so-called r/a-ratio, the ratio of the radius r of the pores and the lattice constant a of the PhC. This is a very important feature which will be very useful for the gas sensor application described below, because it is possible to adjust the PhBS to the different resonance frequencies of various gas under investigation by simply changing the pore diameter.
Furthermore the scale invariance of Maxwell's equations greatly simplifies the necessary computational effort for theoretical studies. After having calculated the PhBS, i.e. the frequency ω and the field distribution $\vec{H}(\vec{r})$, for one set of parameters ϵ, a and r/a, one can easily derive the frequencies ω' and the field new distributions $\vec{H}'(\vec{r})$ after rescaling the PhC by a factor s by using the equations

$$\epsilon'(\vec{r}) = \epsilon(\vec{r}/s) \tag{1}$$

$$\begin{aligned} \vec{H}'(\vec{r}) &= \vec{H}(\vec{r}/s) & (2)\\ \omega' &= \omega/s. & (3) \end{aligned}$$

This scale invariance in addition adds a lot of freedom for designing PhC based gas sensors for a variety of different gases.
In the next section we will discuss the use of PhCs for compact sensing devices.

1.2. Photonic crystals in gas sensors

In many fields such as technical, environmental, automotive as well as medical applications gas sensors are indispensable. The concentration of dangerous and/or air polluting gases such as O_3, NO_x, CO_x, CH_4, C_2H_5OH, etc., occurring in technical processes has to be monitored to prevent harm. In the medical sector it is ,e.g., necessary to monitor and control respiratory gases.
Several types of gas senors are available on the market. One class of gas detectors measures the changes of the conductance or of the capacitance that are induced by the presence of certain gas atoms which are adsorbed onto the surface or diffuse into the detector material. Calorimetric gas sensors measure the change in temperature when certain gases pass by a heated detector. Most of these methods are only applicable to certain specific gases that influence physical properties of the detector materials.
Another class of detectors, the so-called spectroscopy- or optical gas sensors, measures the change of reflection or transmission in the presence of gases. Here, characteristic absorption lines arising from rotational-vibrational excitations of the molecules in the mid-infrared (MIR) spectral range are monitored. This spectroscopic approach is a rather general approach applicable to a broad variety of gases and is in addition highly selective due to the specific rotational-vibrational states (*fingerprint*) for every gas. The major drawback of such optical sensors is their relatively high cost due to the high demands on the optical components.
As an alternative approach we suggest the use of PhCs to obtain compact, robust and low-cost spectroscopic gas sensors.

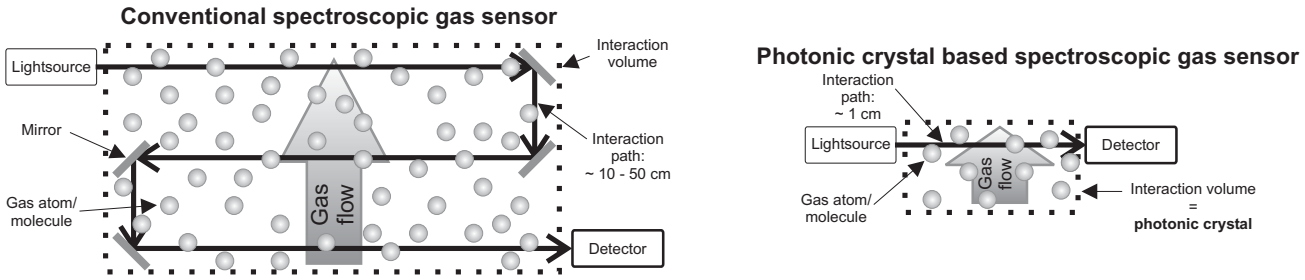

Figure 2. Comparison of a conventional (left) and a PhC based gas sensor (right). The gas sensor size could be drastically reduced using PhCs as interaction volume.

A conventional spectroscopic gas sensor consists of three basic parts: the em radiation source, the interaction volume and the radiation detector. For the moment we only consider the replacement of the interaction volume in such a conventional sensor by a PhC as shown in Fig.2 although one could also think of replacing the em radiation source by a PhC thermal emitter that shows enhanced emission in the spectral region of interest due to the redistribution of the photonic density of states (PhDOS) within the PhC.[3,4,5]

Due to the dilute nature of gases their interaction with light is rather weak which in turn necessitates relatively long interaction paths in the range of 10 to 50cm length for concentrations in the ppb range where the em radiation interacts with the gas. Such long interaction paths and the resulting large interaction volumes, e.g., glass tubes, are rather impractical because first, they result in relatively large sensor devices and second, it is sometimes hardly possible to fill such large volumes with gas, as ,e.g., in the case of baby breath monitoring.

A reduction of the interaction volume can be achieved by increasing the effective interaction of the em radiation and the gas within the interaction volume. Mirrors can be used to multiply reflect the light within the interaction volume and thereby multiplying the interaction between radiation and gas which allows to reduce the interaction volume. Such a versatile construction with elaborate alignment of the mirrors leads to a decrease of robustness, compare Fig.2. Furthermore it is usually necessary to keep the interaction volume at a certain temperature to avoid condensation within the interaction volume and to guarantee reproducible measurement conditions. This is energy consuming, especially for large volumes. In PhCs several factors have to be considered when looking at the gas-radiation interaction.

A closer look on the PhBS reveals that the slope of the PhBS represents the group velocity $\vec{v}_g = \partial\omega/\partial\vec{k}$ for em waves of frequency ω within the PhC, where $\vec{k}$ is a vector in the reciprocal lattice of the PhC. Consequently, in regions where the photonic bands are *flat*, the group velocity $|\vec{v}_g|$ is low. Such a reduction of the group velocity down to about $0.02c$ and $0.05c$ has been experimentally verified for line defects in PhCs by Notomi et al.[6] and Asano et al.,[7] respectively, where c is the speed of light in vacuum. This means that light travelling through the PhC at a lower speed $v_g < c$ interacts longer with the gas, i.e., the interaction time t_{int} is increased and therefore the length of the interaction path l_{int} can be reduced while keeping the total interaction constant. In another simple intuitive picture the low group velocity can be interpreted as a result of the many reflections due to the many scattering surfaces in the PhC. As a consequence the fields of the scattered waves superimpose coherently and interact several times with the gas atoms and this gives the enhanced interaction. From this argument one can deduce that the interaction $I \propto 1/v_g \propto \vec{E}^2$ where $\vec{E}$ is the electric of the incoming plane wave.

Furthermore one has to consider the redistribution of the field energy within a PhC. In a conventional gas sensor the mode that interacts with the gas is more or less a plane wave. In a PhC in contrast, due to the interference of the multiply scattered em waves travelling through it, a lot of mode profiles strongly differing from plane wave field distributions can be observed. For certain frequencies, i.e. in certain photonic bands, some of the modes have the maximum of their field intensity in the high ϵ region (*dielectric bands*), e.g., in the Si matrix, while other modes have their field intensity maxima in the low ϵ regions (*air bands*), e.g., in the air pores.

The interaction I, e.g., the absorption A of em waves of frequency ω travelling through a gas, where ω is one of the resonance frequencies of that gas, is proportional to the Intensity of the redistributed electric field $\vec{E}_{red}$ and

to the interaction time and can be written as

$$Int \propto t_{int}\vec{E}^2_{red} \propto \frac{1}{v_g}\vec{E}^2_{red}. \tag{4}$$

From equation (4) it is obvious that reducing the group velocity v_g and increasing the field intensity $\vec{E}^2_{red}$, as it is possible using a PhC, allows to enhance the interaction of gas and radiation and in consequence to reduce the size of the interaction volume.
In a classical picture a low group velocity v_g corresponds to a high refractive index n_{eff}. Taking into account Fresnel's equations

$$R = \left(\frac{n_2 - n_1}{n_2 + n_1}\right)^2 \tag{5}$$

$$T = \frac{4n_1n_2}{(n_2 + n_1)^2} \tag{6}$$

for the reflected and transmitted part of an em wave entering a dielectric medium with refractive index n_2 from a medium with refractive index n_1 at normal incidence, respectively, a drawback of such a simple PhC based gas sensor emerges. While the high effective refractive index n_{eff} of a flat band helps to increase the interaction between gas and light by reducing v_g, it hampers at the same time in- and out coupling of the em radiation into and out the PhC, respectively. This problem could be overcome by the design of an appropriate taper or an anti-reflection coating.
Because suitability of PhC in gas sensor devices only depends on the specific band structure of the PhC, one can take into account either 2D or 3D PhCs, which will be described in the following part.

2. REALIZATION USING 3D PHOTONIC CRYSTALS

In a first proof of principle experiment 3D PhCs realized in the macroporous Si material system were fabricated and investigated. Numerical simulation using the MIT Photonic Bands software package[8] suggested to use the 3D PhC structure shown on the right side in Fig.3a. The corresponding PhBS on the left side in Fig.3a shows that the upper band edge of the photonic bandgap along ΓA direction coincides with the absorption lines at about $a/\lambda \simeq 0.148$ of the gases used for measurements (NH_3: 972 cm^{-1}; SF_6: 948 cm^{-1}) at the A point of the Brillouin zone depicted in Fig.3b. Due to the non-circular pore shape which is an unavoidable outcome of the etching process the bands are no longer degenerate. This explains the observable splitting of the bands in Fig.3a. According to the parameters used in the simulation lithographically prestructured n-Si wafers were photo-electrochemically etched as described, e.g., by Schilling et al..[9] In the x-y-plane a hexagonal lattice with a lattice constant $a = 1.5\mu m$ was chosen and the diameter of the pores was varied between $(r/a)_{min} = 0.27$ and $(r/a)_{max} = 0.42$ along the z-axis with a modulation period l_z of $3.2\mu m$. An SEM image of the etched 3D PhC can be seen in Fig.3c. The x- and y-components of the electric field for the 3rd and 4th band, respectively, at the A point are shown in Fig.3d. It can be seen that a considerable amount of the energy is concentrated in the air pores and therefore allows interaction with the gas flowing along the pores as schematically shown in Fig.3c. The optimized 3D PhC with 10 modulation periods along the ΓA direction with an airband spectrally overlapping with the SF_6 absorption edge was then characterized using IR spectroscopy. Fig.4a shows the transmission through the 3D PhC under vacuum conditions. The measured high frequency edge of the PhBG corresponds well to the calculated PhBS in Fig.3a. To check for the expected enhanced absorption the transmission through the PhC with SF_6 filled pores was measured and normalized to the transmission with N_2 filled pores. As reference served a 2D PhC, i.e., a Si sample with no modulation of the pores along the ΓA direction, with the same porosity as the 3D PhC to guarantee for the same number of gas atoms in the pores. The results are shown in Fig.4b. No significant difference in the transmission data was found. The rather noisy curve for the 3D PhC results from the low coupling efficiency of the light in and out of the PhC due to the high effective refractive index. Taking eqn.(4) into account the non-occurrence of the enhanced absorption can be explained by the following relations: 1.) The absorption A is proportional to $1/v_g \propto n_{\text{eff}}$. 2.) The transmission T is for large effective indices n_{eff}

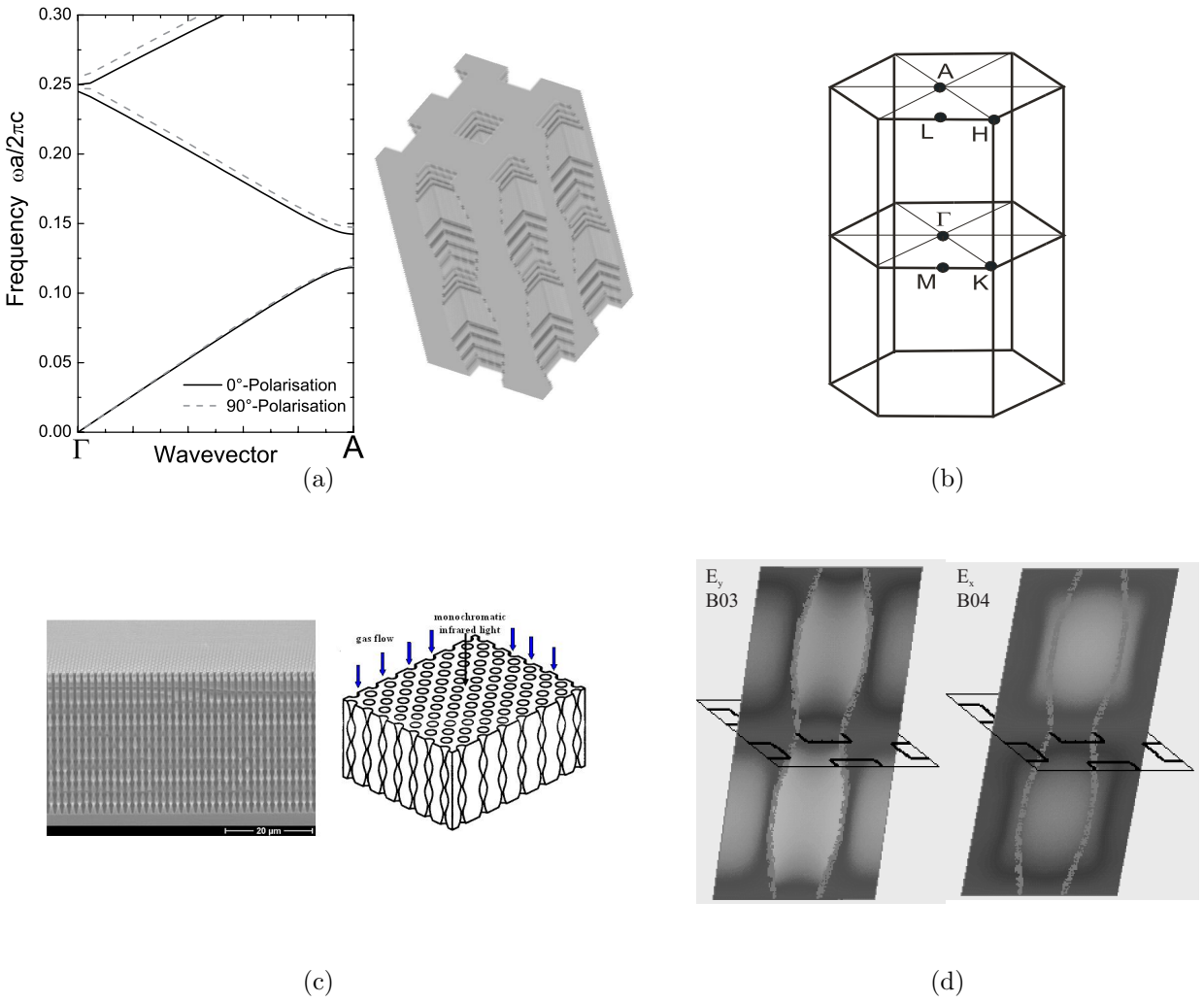

Figure 3. (a) Photonic bandstructure (left) and spatial profile of the dielectric constant ϵ (right) of a 3D PhC made of macroporous Si. The diameter of the air pores is varied along the z-direction, i.e., along the pores, to provide a 3D PhC. Due to the non-circular shape of the pores the degeneracy of the bands is lifted. **(b)** Brillouin zone of the 3D PhC. **(c)** SEM micrograph of the photo-electrochemically etched 3D PhC and measurement principle. Here the light as well as the gas travel along the pore axis. **(d)** Intensity of the x- and y- component of the electric fields for bands 3 and 4, respectively, at the A point of the corresponding Brillouin zone. Bright colors represent high field values.

approximately proportional to $1/n_{\text{eff}}$. So for the measured signal these two effects cancel each other so that no enhanced absorption is observed. Potential effects due to the redistribution of the electric field energy $\vec{E}^2_{red}$ are not taken into account here. To measure the enhanced absorption an improvement of the coupling of light into and out of the PhC a taper is therefore necessary. This issue will be discussed in the next section.

The principle of such a taper for a 3D PhC is shown in Fig.5. To avoid the high reflection when coupling to a flat part of a band, the length of the unit cell along the pore axis is enlarged as shown in the left part of Fig.5. This leads to a shift of the corresponding band towards lower frequencies as depicted in the right part of Fig.5. Now it is possible to couple into the same band, but at a steeper part of that band with a lower n_{eff} and therefore lower reflection loss. Continuous decrease of the lattice parameter l_z to the value necessary for overlap of the bandedge with the gas absorption line adiabatically squeezes the light into the flat region of the band used for gas detection.

Moreover, to compensate for fabrication tolerances which lead to a deviation between the position of the band-

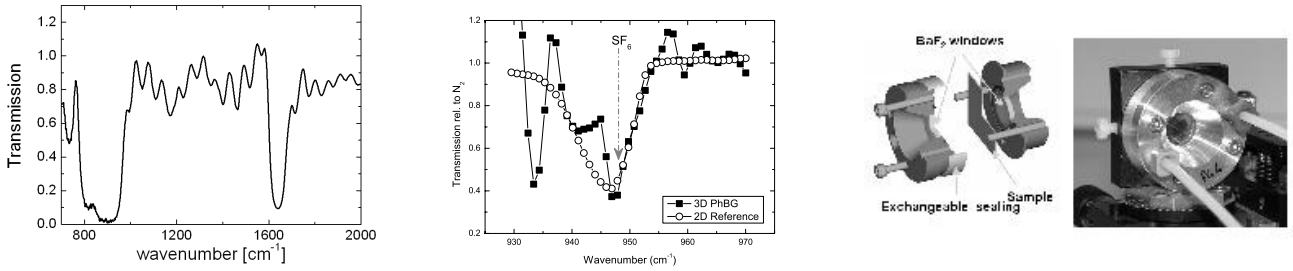

(a) (b) (c)

Figure 4. (a) Transmission through the 3D PhC under vacuum. **(b)** Transmission through SF_6 filled PhCs (normalized to N_2) for a 3D PhC and a 2D PhC with the same porosity. **(c)** Design of the cell used for the measurements.

edge and the gas absorption frequency it is possible to rotate the sample around an axis vertical to the pores. By this means it is possible to shift the bandedge about 35cm^{-1} for a tilting angle of 15°, corresponding to a 4% of the bandedge position and lying within typical fabrication tolerances for macroporous silicon.

3. REALIZATION USING 2D PHOTONIC CRYSTALS

For PhCs solely the periodic arrangement of materials with different dielectric constants is necessary. Therefore various lattices with and without basis atoms (a few examples are shown in Fig.1a-c) can be chosen to yield a bandstructure suitable for use in gas sensor devices. Investigation of several geometries with and without additional basis atoms left a PhC made of air pores arranged in a simple hexagonal lattice in Si as a promising candidate for PhC based gas sensing. The black solid lines in Fig.6a show the bandstructure of a 2D PhC made of macroporous silicon with an r/a ratio of 0.385. At a wavevector near the ΓK_1 point the gas absorption frequency coincides with a flat part of second TE band. The z-component of the magnetic field H_z for that k-point is shown in the lower left panel of Fig.6c. Its symmetry allows for the coupling of a plane wave from outside the PhC to this mode. Furthermore at this k-point the electric field energy (upper left panel in Fig.6c) is concentrated within the pores, i.e., this band is an air band, and therefore allows interaction with gas flowing through the pores. As already described in the case of 3D PhCs for use in gas sensing devices in section 2, flat bands correspond to high effective refractive indices n_{eff} and therefore make it difficult to couple light into those modes. As a solution in the 3D case we introduced a taper concept based on distorting the PhC lattice in a specific way. A similar concept can be used in the 2D case. The point of interest for gas sensor application lies

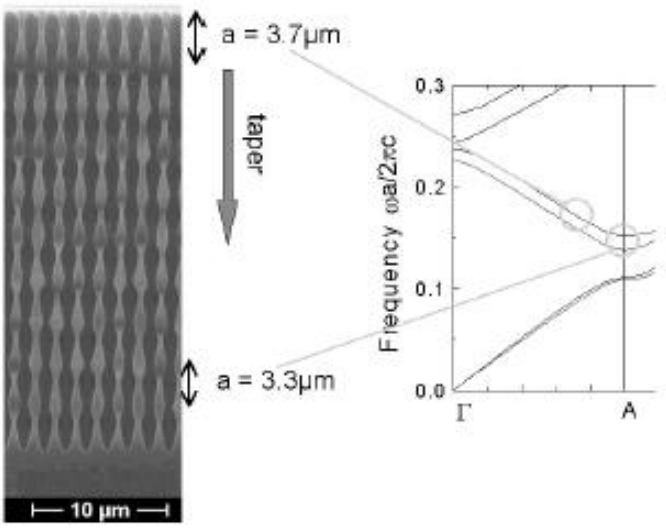

Figure 5. Left: SEM micrograph of a tapered 3D PhC, where the lattice parameter along ΓA was varied. **Right:** Principle of the PhC taper: light is coupled into a *steep* part of the band corresponding to a larger lattice constant l_z than the desired one and then transferred into the *flat* part of the band by changing the lattice constant slowly.

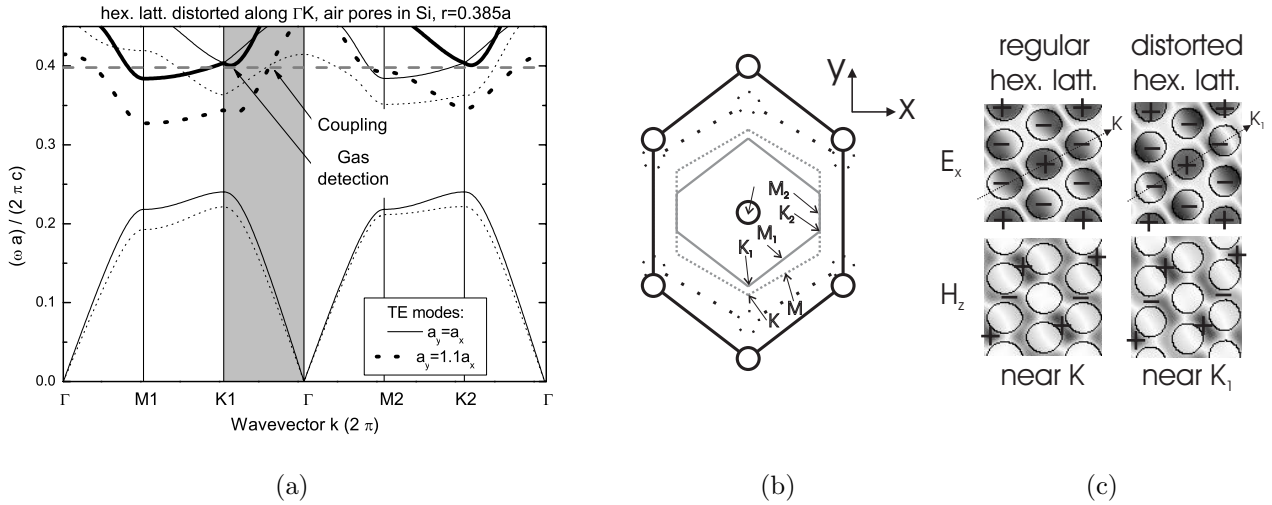

(a) (b) (c)

Figure 6. (a) Bandstructure of a regular 2D hexagonal PhC (solid lines) and distorted hexagonal 2D PhC (dotted lines). The distortion is along the ΓK direction. The horizontal dashed grey line marks the gas absorption frequency. The grey region highlights the k-direction of interest. **(b)** Brillouin zones for a regular and a distorted hexagonal lattice. The threefold degenerate points of high symmetry K and M in the case of the regular lattice have to be replaced by the high symmetry points K_1, M_1, K_2 and M_2. The dotted lines represent the regular lattice while the solid lines stand for the distorted hexagonal lattice. Black lines mark the lattice in real space, and grey lines represent the Brillouin zones for both cases, respectively. **(c)** E_x and H_z fields at the k-point intended for use in gas-sensing applications for regular and distorted hexagonal lattices of air pores in Si. The "+" and "-" denote positive and negative field values. Dark colors indicate high field values. The dotted arrow denotes the direction of distortion.

along the ΓK direction in the regular hexagonal lattice. A distortion of this lattice along that direction leads to a tetragonal symmetry of the unit cell and therefore the high symmetry points M an K in the regular lattice have to be replaced by the high symmetry points K_1, M_1, K_2 and M_2 in the distorted hexagonal lattice with tetragonal symmetry as shown in Fig.6b. This distortion leads as in the case of the 3D PhC to a downshift of the PhBS and therefore allows to couple to a steep part of the 2nd TE mode with correspondingly lower refractive index and lower reflection (compare eqn.(5)). A gradual reduction of the lattice distortion down to the value of the regular lattice should then adiabatically couple the light to the mode at the desired k-point. Comparing the fields of the regular hexagonal lattice in the left panels of Fig.6c with the fields in the right panel representing the case of the distorted lattice shows that the distortion does not have a significant impact on the mode field distribution and therefore adiabatic coupling should work. Regarding this kind of taper one has in addition to take into account that there is a limit in how much the PhC lattice can be distorted. For the situation described above distortions of more than 20% relative to the lattice constant of the regular lattice, the PhBS shifts down too much and it is no longer possible to couple to the desired mode, as shown in Fig.7a. Furthermore one should always try to couple into the steepest part of the interesting band thereby yielding minimal reflection. In the case considered here a distortion of about 10% corresponding to an effective refractive index $n_{\text{eff}} = 3.3$ as can bee seen in Fig.6a. In this context one should also keep in mind that ideally one would like to couple light into only on mode, i.e. working close to the bandedge is favorable. Tapering brings also the risk of coupling into unwanted modes, as it appears to be the case for the 3rd TE band along ΓK_1 in our case. But due to symmetry reasons this band can not couple to an incoming plane wave. Similar to the 3D PhC case, rotation (this time around an axis along the pores) as depicted in Fig.7b allows to shift the bandstructure to compensate for fabrication errors. From an application point of view it might be necessary to make the pore walls chemically inert, e.g., for the detection of aggressive gases. Simulations showed that covering the pore walls with a few tenths of nm SiN do neither significantly influence the PhBS nor the field distributions needed in a PhC based gas sensor.
As mentioned before the interaction volume of a gas sensor might have to be heated. Typical temperatures are on the order of 50-100°C. A temperature change influences both, the dielectric constant $\epsilon_{Si}(T)$, as well as the lattice

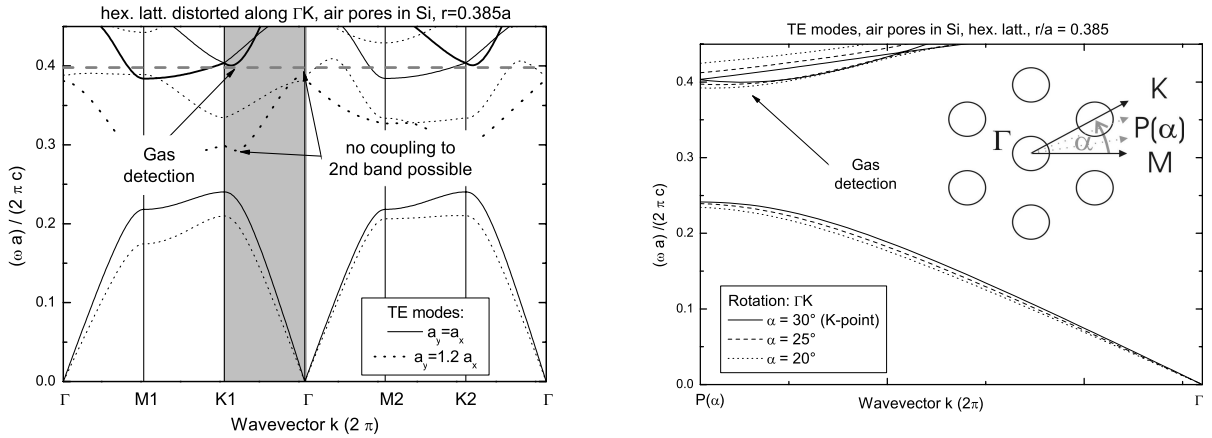

(a) (b)

Figure 7. (a) If the distortion exceeds 20% the bandstructure shifts down too much and coupling to the desired band is no longer possible. The grey region highlights the k-direction of interest. **(b)** Change of the bandstructure along ΓK direction by rotating around an axis along the pores to allow fabrication error compensation.

parameter $a_{Si}(T)$ of the Si crystal, respectively. Taking the thermo-optical coefficient of Si $\delta n_{Si}(T) \simeq 2{\cdot}10^{-4}\mathrm{K}^{-1}$ and assuming a temperature change of 100K reveals that the bandstructure of the PhC shifts only by about $0.005a/\lambda$. And only for temperature changes on the order of several thousand K the bandstructure would shift by about $0.001a/\lambda$ based on the thermal expansion coefficient of bulk Si. This demonstrates that a PhC based gas sensor is rather insensitive to temperature variations which makes it a rather robust design.
Numerical Finite-Difference Time-Domain (FDTD) simulations as well as time-harmonic finite-element solvers (FEM) however showed that using a taper described above to minimize reflection at the AIR/PhC interface does not improve the transmission in the 2D case. This can be understood by comparing the mode profile of an incoming plane wave and the mode intended for use in gas sensing applications. While a plane wave has flat phase fronts with no lateral nodes, the $\vec{E}$ field in the PhC has 2 lateral nodes and a curved phase front. Thus for effective coupling more than just this simple taper only taking the effective refractive index into account has to be used.[10] For the 3D case described in section 2 tapering by stretching the lattice should work, because there the mode profile of the intended band at the A-point of the Brillouin zone is similar to a plane wave. We suggest the use of a special *anti reflection coating (ARC)*[11] as shown in Fig.8a. Our approach is not to be confused with classical $\lambda/4$ layers used to reduce reflection at dielectric interfaces for certain frequencies which would in our case correspond to a thickness of 775nm $\approx 0.185a$ and also shown in Fig.8b. Such a classical $\lambda/4$ layer of Si in front of the first pore row of the PhC in contrast reduces the transmission compared to the bare pore/air interface corresponding to an ARC thickness of $0a$. For the case discussed above the transmission for an untapered PhC is increased from about 18% up to about 47% using an appropriate ARC of thickness $0.6a$. That the suggested ARC is fundamentally different from the classical $\lambda/4$ layer follows from the fact that such a classical anti reflection coating would also work for odd integer multiples of $\lambda/4$. The corresponding ARC thicknesses are shown as dashed vertical lines in Fig.8b. At none of these positions the transmission is extraordinary high. FDTD transmission calculations for other bands with interesting k-points for gas sensing application show that the ARC thickness has to be simulated for each case individually. A further advantage of using an ARC in contrast to an untapered PhC (i.e. $t_{ARC} = 0$) is given by the reduced scattering of light when entering the structure trough a flat, polished surface instead of a surface corrugated by pores.

4. CONCLUSIONS AND OUTLOOK

We presented a new concept for compact gas sensors based on photonic crystals. The interaction between gas and em radiation takes place inside a PC in such a way, that a flat part of an airband of the bandstructure

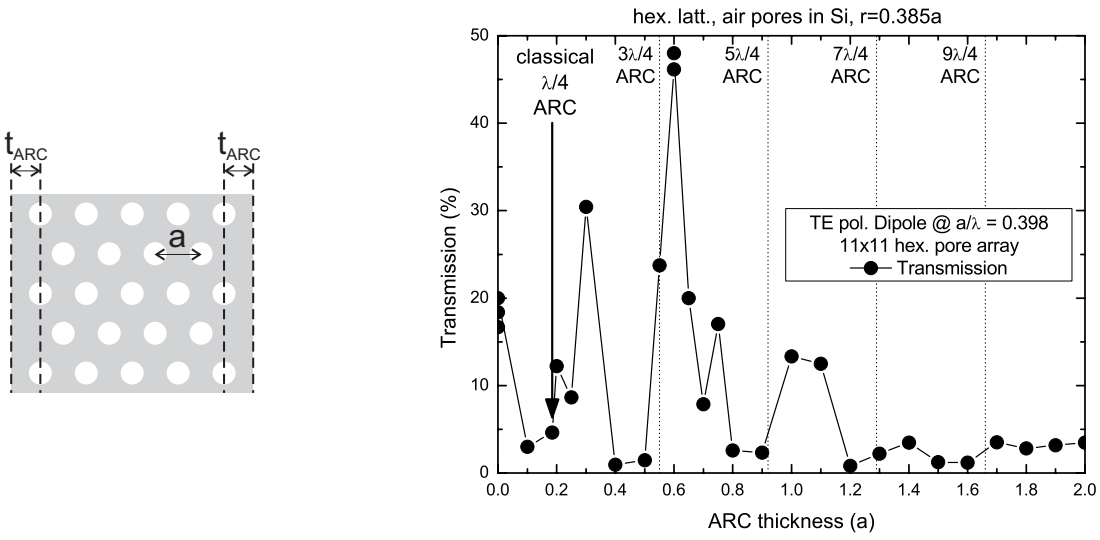

(a) (b)

Figure 8. (a) Principle of the suggested anti reflection coating (ARC) to improve coupling to the PhC. **(b)** Transmission dependance on thickness of ARC through a 2D PhC of hexagonally arranged air pores in Si for $r/a = 0.385$ and $\lambda = 10.55\mu m$. This ARC is not to be confused with a classical anti reflection coating of thickness $\lambda/4$, for which the transmission is indicated. Several runs of the FDTD Simulation with slightly different numerical settings show that the calculated transmission is accurate within $\pm 2\%$.

spectrally overlaps with the absorption frequency of the gas. Due to the low group velocity of the light in flat bands, which corresponds to coherent superposition of fields, the interaction is spatially enhanced which allows a drastic minimization of the interaction volume compared to conventional gas sensors. Due to the scaling invariance of Maxwell's equations a photonic crystal based device can be designed to work for a variety of gases by choosing the material system (resp. the dielectric contrast), the symmetry of the PhC and the lattice constant. Compensation of fabrication tolerances can be achieved by rotation of the sample. Either 2D or 3D photonic crystals can be used. In a first experiment we were not able to verify the interaction enhancement because of the simultaneously increased reflectivity due to the low group velocity. Taper concepts to circumvent this problem have been suggested and will be reviewed in more detail in the near future.

The authors would like to acknowledge financial support by the BMBF within the project PHOKISS (13N8525).

REFERENCES

1. S. John, "Strong localization of photons in certain disordered dielectric superlattices," *Physical Review Letters* **58**(23), p. 2486, 1987.
2. E. Yablonovitch, "Inhibited spontaneous emission in solid-state physics and electronics," *Physical Review Letters* **58**(20), p. 2059, 1987.
3. S. Y. Lin, J. G. Fleming, E. Chow, J. Bur, K. K. Choi, and A. Goldberg, "Enhancement and suppression of thermal emission by a three-dimensional photonic crystal," *Phys. Rev. B* **62**, p. R2243, 2000.
4. J. G. Fleming, S. Y. Lin, I. El-Kady, R. Biswas, and K. M. Ho, "All-metallic three-dimensional photonic crystals with a large infrared bandgap," *Nature* **417**, p. 52, 2002.
5. M. Pralle, N. Moelders, M. McNeal, I. Puscasu, A. Greenwald, J. Daly, E. A. Johnson, T. George, D. Choi, I. El-Kady, and R. Biswas, "Photonic crystal enhanced narrow-band infrared emitters," *Appl. Phys. Lett.* **81**(25), p. 4685, 2004.

6. M. Notomi, K. Yamada, A. Shinya, J. Takahashi, C. Takahashi, and I. Yokohama, "Extremely large group-velocity dispersion of line-defect waveguides in photonic crystal slabs," *Phys. Rev. Lett.* **87**(25), p. 253902, 2001.
7. T. Asano, K. Kiyota, D. Kumamoto, B.-S. Song, and S. Noda, "Time-domain measurement of picosecond light-pulse propagation in a two-dimensional photonic crystal-slab waveguide," *Appl. Phys. Lett.* **84**(23), p. 4690, 2004.
8. S. Johnson and J. Joannopoulos, "Block-iterative frequency-domain methods for maxwell's equations in a planewave basis," *Opt. Express* **8**(3), p. 173, 2001.
9. J. Schilling, F. Müller, S. Matthias, R. B. Wehrspohn, U. Gösele, and K. Busch, "Three-dimensional photonic crystals based on macroporous silicon with modulated pore diameter," *Applied Physics Letters* **78**(9), p. 1180, 2001.
10. J. Witzens, M. Hochberg, T. Baehr-Jones, and A. Scherer, "Mode matching interface for efficient coupling of light into planar photonic crystals," *Phys. Rev. E* **69**, p. 046609, 2004.
11. A. v. Rhein, T. Geppert, D. Pergande, and R. B. Wehrspohn, "Efficient mode coupling for 2d photonic crystals using a modified anti-reflection coating," *in preparation* , 2004.